Czech University of Life Sciences
Faculty of Environmental Sciences

Landscape Engineering - Landscape Planning

Urban Heat Island Effect in Prague: Remote Sensing Approach

Diploma Thesis

Author: Tugba Dogan
Thesis supervisor: Ing. David Moravec

Prague 2017

CZECH UNIVERSITY OF LIFE SCIENCES PRAGUE

Faculty of Environmental Sciences

DIPLOMA THESIS ASSIGNMENT

B.Sc. Tugba Dogan

Landscape Planning

Thesis title

Urban Heat Island Effect in Prague: remote sensing approach.

Objectives of thesis

This diploma thesis addresses the topic Urban Heat Islands Effect in Prague. Determining and evaluating Urban Heat Islands effects according to this objectives:

1) Literature review of UHI phenomenon.

2) Analysis of the spatial distribution of Land surface temperature (LST) and its relationship with Normalized Difference Vegetation Index (NDVI)using Landsat 8 TIRS and OLI satellite images.

3) Determine of Urban Heat Island effect in Prague according to foregoing analysis.

Methodology

1)Selecting and downloading the most appropriate image on the basics of Prague meteorology condition in the year of 2016 and cloud free image availability.

2)Satellite image pre-processing (atmospheric correction, orthorectification).

4)Extraction of temperature and NDVI values.

5)Analysis relationship between LST and the NDVI (Normalized difference vegetation index).

The proposed extent of the thesis

According to need

Keywords

Temperature; Thermal Infrared; NDVI; Urbanization

Recommended information sources

Arnfield, A.J. (2003) 'Two decades of urban climate research: A review of turbulence, exchanges of energy and water, and the urban heat island', International Journal of Climatology, 23(1), pp. 1–26. doi: 10.1002/joc.859.

Byles, J. (2017). How to beat extreme heat: Strategies for combating the urban heat island effect — Broken Sidewalk. [online] Broken Sidewalk. Available at: https://brokensidewalk.com/2016/urban-heat-island-effect/ [Accessed 24 Mar. 2017].

Yuksel, U.D. (2015) A study on determining and evaluating summertime urban heat islands in Ankara and local scale utilizing remote sensing and meteorological data. PHD thesis.

Expected date of thesis defence

2016/17 SS – FES

The Diploma Thesis Supervisor

Ing. David Moravec

Supervising department

Department of Applied Geoinformatics and Spatial Planning

Electronic approval: 5. 4. 2017

doc. Ing. Petra Šímová, Ph.D.

Head of department

Electronic approval: 5. 4. 2017

prof. RNDr. Vladimír Bejček, CSc.

Dean

Prague on 19. 04. 2017

Declaration

I hereby declare that the work presented in this thesis is, to the best of my knowledge, original work, except as cited in the text. The research was completed under the direction of Ing.David Moravec.

Prague, 2017 Tugba Dogan

Acknowledgment

I would like to thank my supervisor, Ing. David Moravec, for the patient guidance, encouragement and advice he has provided throughout my time as his student. His positive outlook and confidence in my research inspired me and gave me confidence. I have been extremely lucky to have a supervisor who cared so much about my work, and who responded to my questions and queries so promptly. His careful editing contributed enormously to the production of this thesis.

Abstract

This thesis will focus on determining and evaluating the effects that Urban heat islands (UHI) has on Prague by using a remote sensing approach. Analysis will be provided on the spatial distribution of Land Surface Temperature (LST) and its relationship with Vegetation density calculated by an index known as Normalized Difference Vegetation Index (NDVI) using thermal remote sensing data. Both ENVI 5.3 and ArcGIS 10.2.1 Software were used to process the Landsat 8 TIRS and OLI satellite images. In order to examine the relationship between NDVI and LST, 900 random points were created with ArcGIS and correlation analysis was performed with Microsoft Excel. In order to gain a detailed understanding regarding the NDVI and LST relationship, 18 sites different sites were selected due to several key similarities and differences, with the results being analyzed.

The findings of this thesis show that the UHI phenomenon was mainly observed in the city center, in industrial areas, and at Vaclav Havel Airport in Prague. On the hottest summer day of June 2016: the highest surface temperature observed was at Stadium (O2 Arena) with (48.71 °C) and 0.12 NDVI value on the contrary to that the lowest surface temperature was observed in the agricultural area (29.30 °C) with 0.61 NDVI value. Moreover, a strong inverse relationship was found between NDVI and LST. The analysis of NDVI and LST expressly show that the decrease in vegetation density causes a decrease in the evaporative cooling and consequently coincides with high LST.

Finally, this thesis concludes with recommendations based on the spatial distributions of the UHI and vegetation cover which proved as a main driver of UHI in Prague and its potential to combat UHI. The findings of this thesis can effectively incorporate further analysis of UHI using a multitude factors, and in doing so provide guidance for urban planners and decision makers in their assessment of how to effectively engage with the mitigation measures around Prague.

Key words : Temperature; Thermal Infrared; NDVI; Urbanization

Abstrakt

Tato práce se zaměřuje na určování a hodnocení městských tepelných ostrovů (UHI) v Praze s využitím metody dálkového průzkumu Země. S využitím údajů o teplotě z dálkového průzkumu byla analyzována prostorová distribuce teploty povrchu země (LST), dále byl spočítán její vztah k hustotě vegetace, který byl vyjádřen jako Normalizovaný diferenční vegetační index (NDVI). Ke zpracování satelitních snímkůLandsat 8 TIRS a OLI byl použitý software ENVI 5.3 a ArcGIS 10.2.1. Pro vyjádření vztahu mezi NDVI a LST bylo vytvořeno 900 náhodných bodů a užitím ArcGIS a dále byla provedena korelační analýza s použitím Microsoft Excel. Pro detailní přehled vztahu NDVI a LST bylo vybráno 18 oblastí na základě klíčových podobností a rozdílů a výsledky byly analyzovány.

Výsledky této práce ukazují, že fenomén UHI je pozorován zejména v centru města, průmyslových oblastech a pražském letišti. Navíc byl zjištěn silný vztah mezi NDVI a LST. Analýza NDVI a LST jednoznačně ukazuje, že pokles hustoty vegetace způsobuje pokles ochlazujícího výparu a zároveň vede k vysokému UHI.

Závěry této práce mohou být efektivně použity pro další analýzy UHI s rozdílnými faktory a také plánovači městského rozvoje a lidmi s rozhodovací pravomocí, kteří budou tvořit budoucí rozvoj a určovat zmírňující opatření v Praze.

Klíčová slova:

Teplota, Termální spektrum, , NDVI, Urbanizace

TABLE OF CONTENTS

1. INTRODUCTION

Urban climate is a local climate that is altered by interactions between structured areas (including heat pollution and air pollutant emissions) and regional climate (WMO,1983). A city's climate is a local mesoclimate with a spatial extent of about 250 km (WHO 2004).

The Urban climate has been subject of study dating back to at least to the Classical Era of the Roman Empire. Vitruvius (B.C. 75-26) went on great length regarding the climatic conditions and urban planning of Roman Cities. Main topic of urban climate had been urban planning and air pollution from Roman Cities to till the beginning of the 17th century. Qualitative researches about urban heat island and heat balance have started the end of the 17th century. (Yuksel, 2015). 18th to 19th centuries with the Industrial Revolution, urbanization increased and caused to distinctive alteration of the urban climate (Yuksel, 2015). In early 19th century British chemist Lake Howard examined urban climate in London and he is the first person to measure and discuss urban heat island effect (Yang et al., 2016). As OKE (1987) describes Urban Heat Island phenomenon (UHI) in the urban area air temperature is higher than its surrounding area and it refers to temperature characteristic of urban area (Oke,1995)

Such directly impacts more than half of the world's population lives in urban area and, by 2050, 66% of the world's population is predicted residing in urban areas (United Nations, 2014, Small, 2006) To accommodate such amount of the urban population growth, urban infrastructure, buildings, need to be developed causing to rapid changes in land use patterns. Due to rapid and unplanned alteration of the land cover, UHI can be severe and threatened the risk of the people especially elderly and young population. For instance, The Centers for Disease Control and Prevention estimates that from 1979-2003, in the USA, due to extreme heats, 8000 people died that is more than hurricanes, lightning, tornadoes, floods, and earthquakes combined (C2es, 2017).

Presently, the Urban Heat Island is one of the most extensively discussed climate-related topics given its strong correlation with climate change and population growth which are increasingly severe environmental problems facing humanity in the 21st century (Stewart and Oke, 2012)

The purpose of this thesis is to determine and evaluate the UHI effects in Prague by using a remote sensing approach. Analysis of the spatial distribution of Land Surface Temperature (LST) and its relationship with Vegetation density calculated by an index known as Normalized Difference Vegetation Index (NDVI).

Based on knowledge from literature review, methodology and analysis were applied. Both ENVI 5.3 and ArcGIS 10.2.1 Software were used to process the Landsat 8 TIRS and OLI satellite images. In order to examine the relationship between NDVI and LST, 900 random points were created with ArcGIS and correlation analysis was performed with Microsoft Excel. In order to gain a detailed analysis regarding the NDVI and LST relationship, 18 sites different sites were selected due to several key similarities and differences, with the results being analyzed.

2. GOALS / AIMS

The aim of this thesis is to determine and evaluate the Urban Heat Islands effects in Prague. Furthermore, the analysis of the spatial distribution of Land Surface Temperature (LST) and its relationship with NDVI will be assessed and scrutinized.

The main outcome intended for this thesis will be based on the literature review, processing thermal remote sensing data and the analysis, to identify the spatial disturbances of UHI in Prague and its relationship with vegetation density (NDVI).

The hypothesis of this thesis was based on the premise that the land surface temperature can gradually increase in Prague due to urban growth and decreasing greenery.

3. LITERATURE REVIEW

3.1. Urban Heat Island Phenomenon

Urban Heat Island Phenomenon is described as relatively high temperature in the urban area compared to the surrounding rural area (Oke, 1982; Voogt and Oke, 2003) Main driver of the UHI is urbanization. Due to urbanization, natural land cover is replaced by artificial surface and amount of the anthropogenic heat increased (vehicle's, heating -cooling energy)(Streutker 2003).

Consequently, this altering natural surface is cause to breakdown the natural ecological cycles in the city. Therefore, evaporation is decreased, more shortwave and longwave radiation absorbs and wind blocks by built up area and overall temperature is increased in the city (Senanayake, I., at el 2010 : Mirzaei at el., 2010). However, holly unplanned and completely mismanaged cities are more vulnerable to the UHI due to amount of environmental degradation (Kikon et al., 2016).

Even Though UHI effect occurs throughout all the seasons of the year, its existence during the summer in warm climate cities, is a matter of immense public policy concern due to increasing exposure of high summer temperatures which precipitates a rise in air conditioning demand, an increase in air pollution, and a spike in heat-stress related mortality and illness (Rosenfeld et al., 1995)

3.2. Causes of Urban Heat Island

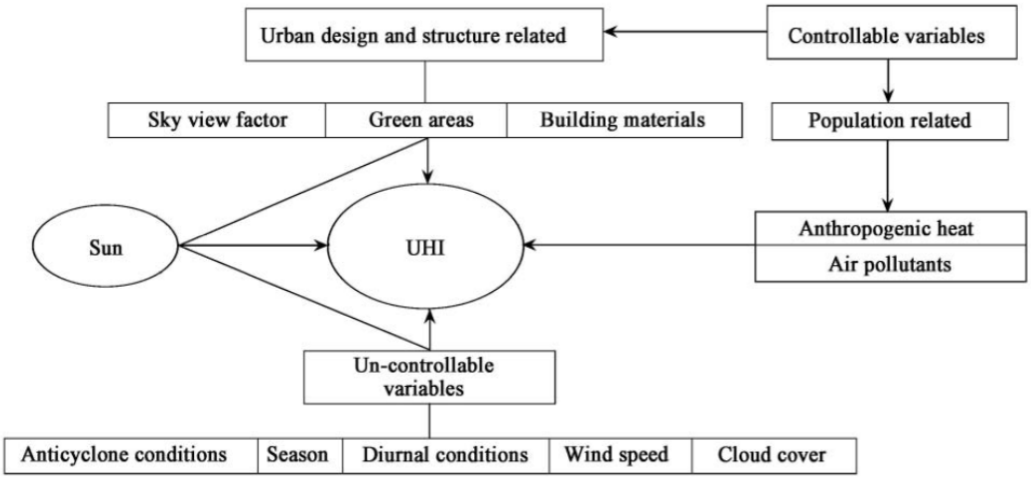

Figure 1. Generation of UHI (Rızwan A, at el, 2017)

Rızwan A. (2017) categorized the various factors involved in the generation of UHI: as either controllable or uncontrollable. The controllable factors are mostly pertaining to design and planning related matters, which can be directly influenced and controlled to some degree, while on the other hand, uncontrollable factors are environment and nature-related which are beyond humanity´s capacity to control.

3.2.1 Uncontrollable Variables

Natural Factors

Geographical latitude, climate, geographic location (on a mountain or in a valley), topography (elevation, landforms) and meteorological conditions (wind, cloud, humidity, sunlight, precipitation etc.) are important factors for UHI and they create unique characteristics for each city. Wienert (2001) in his study on urban heat island of 150 cities found that UHI directly correlates with geographical latitude, acts because of anthropogenic heat generation, the radiation equilibrium and its annual variability change in consonance with latitude. Furthermore, Wienert mentions, that in higher latitudes, the greatest differences between urban and rural environments are greater, than in the lower latitudes. Based on the evidence, correlating with the

discoveries made by Oke (1973) based solely on the necessity of obtaining territories with approximately equal geographical latitude (Koppe et al., 2004).

Gedzelman et al. (2003)'s findings in New York lend support to the claim that UHI depends on cloud cover, wind speed and wind direction. Voogt and Oke (2003) in their study found that enhancing clouds, not only diminish radiative cooling at night, but also lessen the UHI. (Wang ,2016). Moreover, during the time of the calm winds and clear skies, UHI may be intensified city, whereas the opposite effect occurs during time of strong winds and increased cloud cover (Che-Ani, at el 2009). Its proven that the UHI effects are more pronounced in conditions of atmospheric balance, rather than under conditions of imbalance (Alonso, at el 2003)

Water bodies of significant size have been proven to alter surrounding weather (Kusaka et al., 2000). UHI intensity has decreased due to evaporation, whenever there is body of water, which is part of the urban surface. The "Lake Breeze" effect, which is caused by winds coming from the lake to shore, neutralizes the high summer temperatures near Lake Ontario (Scott and Huff, 1996).

Albedo and urban surface materials

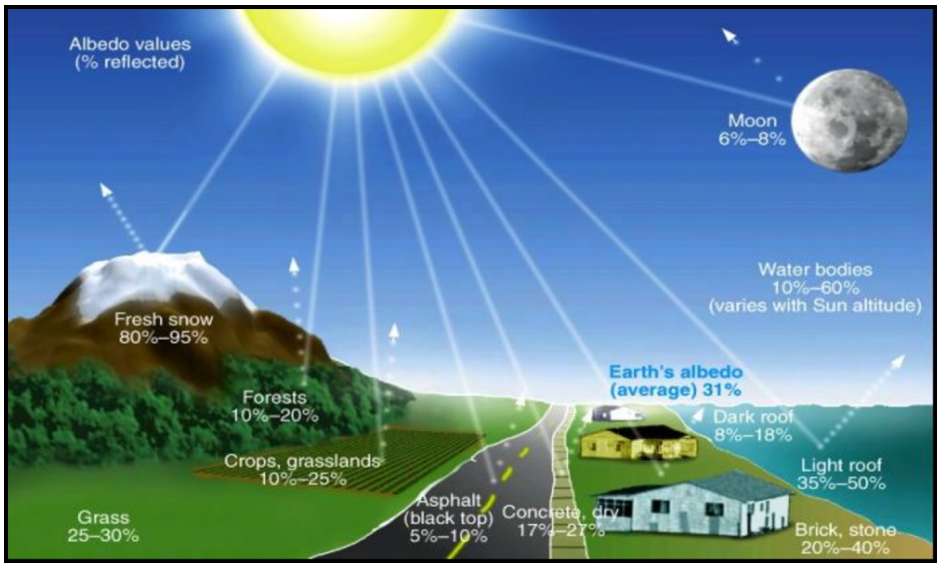

Figure 2. Albedo rates of objects (Regentsearth, 2017)

Due to changing land cover vegetation to impervious surface and building materials which have varied thermal (heat capacity and thermal conductivity) and radiative

(reflectivity and emissivity) properties contrast to countryside, the thermal, radiative, moisture and aerodynamic features of the surface and the atmosphere are changed (Thegreencity, 2017)

Albedo is defined as the ability to reflect sunlight. Light-colored items tend to reflect more efficiently than other items on the visible portion of the spectrum. The scale of 0 and 1 are used to show the amount of light reflected, when measuring albedo. (Urbangreenbluegrids, 2017). Earth reflects about ⅓ of the radiation back into space, with a median albedo for Earth of .31. There are many varieties of albedos for forest, oceans, cities and deserts. An albedo of .30 is common for deserts; whereas an albedo ranging from .08 to .15 is common for forests. (Esseacourses, 2017**)** The roof tops, the walls of high rise structures with darker surfaces, parking lots, roads, pavement constructed with asphalt, and concrete tend to have low albedos (Senanayake, at el 2013). Moreover, these dark low-albedo surfaces absorb a higher amount of solar radiation and convert it to thermal energy (Senanayake, at el 2013).

Moreover, Heat island arise when the impervious surface area of a city exceeds 35 percent. (New York City is about 72 percent impervious.) Forested areas, which are being paved over in sprawling cities, double the rate of compact metropolitan areas, and cause an extreme heat event at twice the rate. (Byles, 2017)

3.2.2 Controllable Variables

Urbanization and Anthropogenic Heat

Its widely accepted and proven that urbanization can have a remarkable influence on regional weather and climate (Landsberg 1981). Urban population is continuing to grow and it is estimated that by 2017, even in less developed countries a majority of people will be living in urban areas (WHO, 2015).

The urban atmosphere has a higher pollution load than the rural areas surrounding it. Pollution, especially aerosols, can create a false greenhouse effect by absorbing long-

wave radiation, reflecting it, and preventing surfaces from cooling by radiation (Streutker 2003).

Essential anthropogenic heat sources that conduce UHI are fossil fuel usage for vehicles and heating / cooling of built infrastructure. (Sailor & Lu, 2004). Moreover, due to anthropogenic reasons increase of temperature related on the function of structure insulation. (Arnfield, 2003). Anthropogenic factor effects on UHI also depend on the size, population and climate conditions of the area so it has a less impact on small town than metropoles. (Oke, 1982).

Urban geometry

Size, shape, composition, and neighborhood planning effect the UHI (Chen et al., 2006). The reduction in air circulation and the overall decrease in the temperature within cities are predominantly caused by skyscrapers and cramped streets, which trap heat accumulated throughout the day (Bokaie et al., 2016).

Assembled thickness and manufactured shape are composite factors consolidating parameters, for example: areas of uncovered outer surfaces, the thermal capacity and surface reflectance of fabricated components, and the perspective of sun and sky by surfaces (Koppe et al., 2004).

Undeveloped ground, receives three times less annual radiation than a cubical structure does. Rural areas usually have higher wind velocities than that of cities. Due to this, convective cooling is less effective thus lowering the rate of heat dissipation. Convoluted airflow patterns and turbulence are a result of the channeling effect of urban canyons, which are formed by tall buildings (Koppe et al., 2004).

Sky View Factor (SVF), the proportion of the sky “viewed” from a fixed spot, is a frequently studied part of urban geometry. An open space parking lot with small amounts of stuff blocking the view would have a high SVF, but an urban canyon would have a low SVF, due to the tall buildings. This SVF is a reason for increased

urban heat islands in cities, because radiation accumulated daily cannot escape to the open sky because of tall buildings that trap the radiation. In the two urban centers of Japan, Fuchu and Higashimurayama, there is a correlation amidst air temperature and SVF (Yamashita et al., 1986).

Lack of vegetation

Vegetation has important ecological services such as evapotranspiration, humidification, shade, and storm water management which serve to decrease the temperature in that region. Therefore, due to a disruption of this ecological services and natural cycle, the urban's temperature is much higher than the temperature found in rural locales. (EPA, 2008)

3.3. Urban Heat Island Types

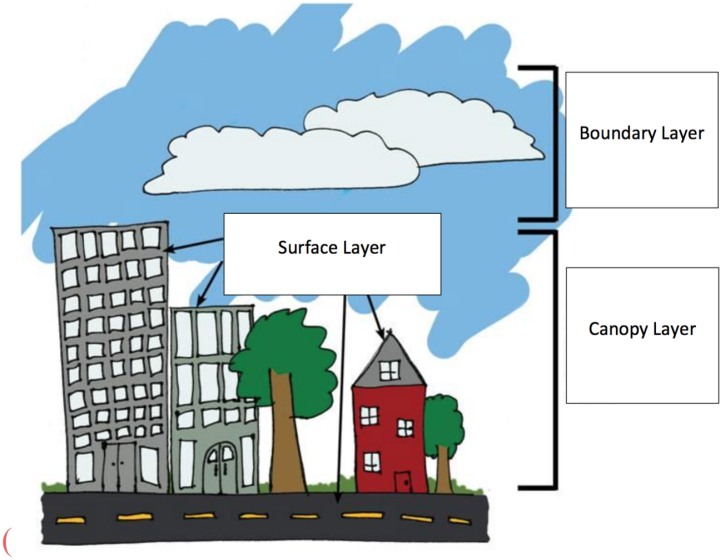

Figure 4. Urban Heat Island Layers Source: EPA (2008)

Heat islands are divided primarily into two categories; Surface Urban Heat Island (SUHI) and Atmospheric Urban Heat Island. Atmospheric Urban Heat Islands are also divided into two subcategories; Urban Canopy Layer (UCL) and Urban Boundary Layer (UBL) (Oke 1976).

3.3.1. Atmospheric Urban Heat Islands

Urban Canopy Layer (UCL) can be described as a layer of urban atmosphere, which generally spans from the surface of buildings of roughly average elevation, which people inhabit, to the peaks of trees and roofs (Voogt and Oke, 2003l) UCL is affected by a subjacent urban surface and perceived to be unaffected by sensors at classical (screen-level) meteorological elevation or from crossing transportation attached sensors (Voogt and Oke, 2003).

Urban Boundary Layer (UBL) can be described as a layer above the UCL, roughly spanning from the apex of average building elevation, to urban landscapes, which are influenced by the atmosphere, and expand no more than 1.5km from ground. (Voogt and Oke, 2003).

Radiosonde or tethered balloon flights, as well as more customized sensor platforms like high towers or from airplane-attached equipments are used for measuring UBL heat island. (Voogt and Oke, 2003).

3.3.2. Surface Urban Heat Islands

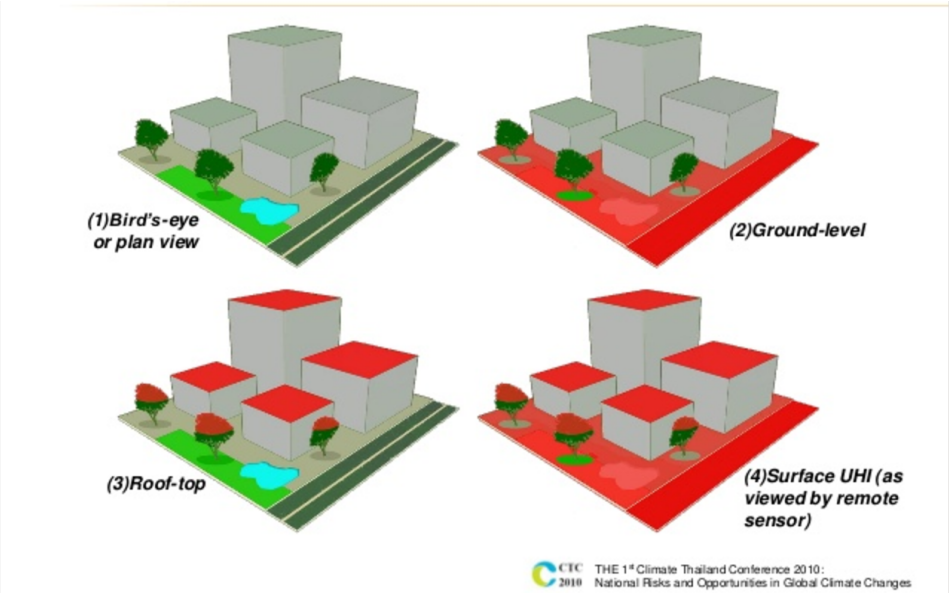

Figure 5. Surface Urban Heat Island
(The 1st Climate Thailand Conference 2010: National Risks and Opportunities in Global Climate Changes /Chiang Mai)

Surface Urban Heat Island (SUHI) imply a temperature distinction perceived by the surface of urban areas, and are also entitled remotely sensed UHI because besides of the other directly measurement options such as meteorological stations, unaffected location measurements; SUHIs can also be measured indirectly with thermal remote sensors from airplane or satellites. (Cochran, 2014)

3.4. Impacts of UHI

UHI has regional-scale impacts on energy demand, air quality, greenhouse gases, water quality, public health and comfort (Voogt, 2002).

Surface temperatures rise during daytime, less so during evening once it begins to cool down, increased air pollution resulting in common annoyances, breathing difficulties and sickness such as heat stroke, tiredness, and fatalities are among the effects that UHI has on urban centers. These variable temperature fluctuations are

more concerning for the vulnerable population such as elderly and younger people (Epa.gov, 2017).

The data appears to suggest that poor water conditions, rising energy expenditures, the disruption of the physical well-being and overall livelihood of people, and an increase in air contaminants and greenhouse gasses are complications associated with UHI. (Voogt, 2004; EPA, 2008). Many related fields such as urban climatology, urban planning, urban geography, and urban ecology have begun to study UHI because of its far-reaching impacts on city life and city ecological environment. (Estoque, at el 2017)

Heat stroke, heat cramps, dehydration, and heat related death are all an acute issue resulting from high heat. During the 2003 Heat Wave, over 15000 people died just in France, with a further 70000 in Europe. (Fouillet et al., 2006) In 1995 more than 739 people perished in Chicago. (Whitman et al., 1997) Cases of Heat Stroke skyrocket, as there is a demonstrable negative impact on the overall well being of the population during heatwaves (Argaud et al., 2007).

Photochemical smog is caused by the evaporation and intermingling of contaminants from urban surfaces which stem from UHI. Due to UHI exacerbating extreme he contamination of drinking water due to thermal pollution is worrisome. Dirt, heat and toxic material are collected by rain water and washed in rivers due to impervious surfaces (Krause et al., 2004; Finkenbine et al., 2000).

On the other hand, The Intergovernmental Panel on Climate Change (IPCC) has proved that UHI effects on local climate appear to include alters in precipitation, clouds, and the daily temperature. (Epa.gov, 2017)

3.5. Remote Sensing of UHI

The total amount of the energy incoming to the earth implied as total radiance. From the electromagnetic spectrum, total radiance reaches mostly in the form of visible and infrared light, with a smaller rank of it being in short wavelength UV, x-ray, and gamma frequencies, besides that in longer wavelength frequencies, like as microwaves (Climate.ncsu.edu, 2017 ; Harris Geospatial Solutions, 2017)

The incoming Sun's radiation should inherently turn to the space to keep in order global average temperature stable. The process of the equilibrium between incoming and outgoing radiation referred the Earth's energy balance. Figure…. As it shown on the Figure, half of the incoming radiation absorbed by earth, the rest is absorbed by cloud and atmosphere. However even the amount of the absorbed radiation less than earth, clouds reflected more than earth (Climate.ncsu.edu, 2017)

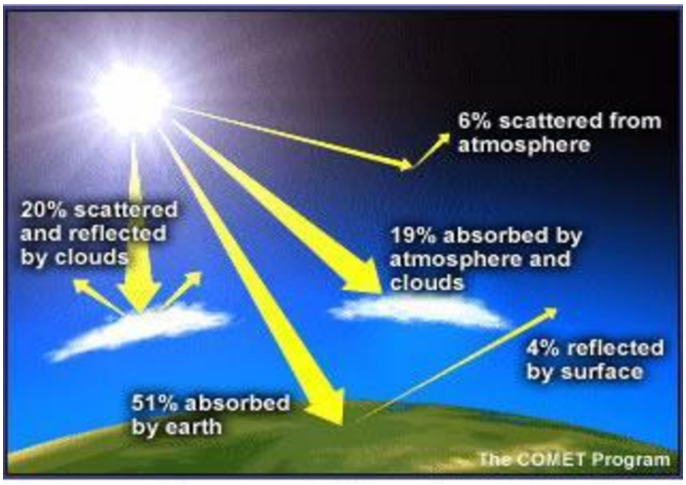

Figure 6. Earth's Energy Balance (Climate.ncsu.edu, 2017)

Infrared remote sensing utilizes infrared sensors for expose infrared radiation which emanates from the Earth's surface. The middle-wave infrared (MWIR) and long-wave infrared (LWIR) are within the scope of the thermal infrared interval. Such radiation is emitted from warm objects such as the Planet's crust. Nevertheless, these radiations are applied in satellite remote sensing measurements of the Earth's land and sea surface temperature. In the electro, magnetic spectrum (Fig.7), belong the

infrared region, the thermal infrared 8-14 µm wavelength interval is mostly used for interest for thermal remote sensing. (Crisp.nus.edu.sg, 2017)

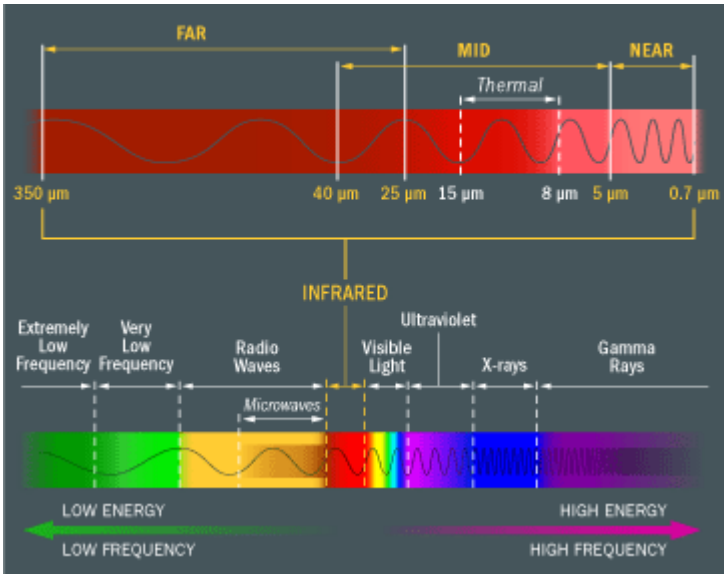

Figure 7. Infrared Region of Electromagnetic Spectrum (HowStuffWorks, 2017)

Before Rao's 1972 Study pioneering the usage of satellite imagery and telemetry to study UHI, all examination was conducted was based off ground based observations of LST. (Voogt and Oke, 2003) Utilizing satellite data effectively, strongly aides in carrying out fruitful investigations on UHI, while also going a long way towards gaining a deeper understanding of the spatial patterns associated with UHI. On the other hand, conducting comparative studies on various urban areas does allow for a more uniform view, one with a greater degree of understanding in analyzing larger scale heat islands. By utilizing remote sensing method, its possible to examine information using the remote sensing method, as it contributes towards gaining a better understanding of the immensity of LST of the city and spatial disturbance of the UHI effect (Epa.gov, 2017).

Nevertheless, the usage of satellites does come with drawbacks. First of all, satellites are incapable of receiving telemetry based off radians, and they are also unable to receive radiant emissions from all urban surfaces (as they are limited to a bird's-eye view): and are limited to solely horizontal surfaces, such as roofs. Given this issue, radiant emissions from vertical surfaces such as walls, are not taken into account.

Secondly, the accuracy of satellite data is variant on prevailing weather conditions and patterns. For example, cloud cover is an important factor in order to select the right satellite image. Finally, since captured radiation passes through the atmosphere twice; consequently, the the scattering and absorption effects from atmosphere are mitigated. Therefore, to accurately estimate solar reflectance and temperatıre, satellite imagery needs further clarification, in order to be processed. (Epa.gov, 2017)

IDRISI, ERDAS IMAGINE and ENVI are the most popular remote sensing softwares to process satellite images. In order to conduct an effective study on UHI, the usage of thermal satellites is a game changer. The most common satellites are those which possess high resolution thermal imagery, and include: Landsat-5 ™ and 7ETM+ and the Satellite Advanced Spaceborn Thermal Emission and Reflection Radiometer (TERRA ASTER) provide LST at a high spatial resolution of 120m and a relatively frequent 16-day pass cycle (USGS,2016, Harris Geospatial Solutions, 2017). Satellites with a lower degree of resolution; ~1km thermal bands, also include Moderate-Resolution Imaging Spectroradiometer (MODIS) and Advanced Very High Resolution Radiometer (AVHRR) which are selected for their high temporal resolution providing twice the daily Land Surface Temperature (LST) imagery. (Stathopoulou, 2009).

On February 11, 2013, the Landsat 8 was launched with two instruments: The Operational Land Imager (OLI) and the Thermal Infrared Sensor (TIRS). The Landsat 8 satellite is capable of capturing entire images the of Earth every sixteen days. The ideal selection criteria associated with satellite sensors, must be taken into consideration, in order to study a wide range of topics. From the aspects of a spatial scale, previous studies of UHI, which use AVHRR or MODIS data are only suitable for large-area urban temperature mapping, not for accurate and meaningful evaluation (Weng, 2009). The Landsat TM (and later ETM+ and OLI/TIRS) and ASTER data have been used extensively to study UHI, given its medium resolution TIR data. Better spatial resolution is preferred when studying UHI at the microscale. (USGS,2016, Harris Geospatial Solutions, 2017)

have been accumulating images of Earth's surface. By meticulously measuring the wavelengths and intensity of visible and near-infrared light reflected by the land surface back up into space, scientists are able to use an algorithm called a "Vegetation Index" to quantify the concentrations of green leaf vegetation around the globe. Chlorophyll, a pigment in plant leaves, strongly absorbs visible light (from 0.4 to 0.7 µm) during photosynthesis. However, the cell structure of the leaves, strongly reflects near-infrared light (from 0.7 to 1.1 µm). Consequently, the more leaves a plant has, the more these wavelengths of light are affected (Earthobservatory.nasa.gov, 2017).

NDVI is calculated from the visible and near-infrared light reflected by vegetation. Healthy vegetation (left) absorbs most of the visible light that hits it, and reflects a large portion of the near-infrared light. Furthermore, unhealthy or sparse vegetation (right) reflects more visible light and less near-infrared light. The numbers on the figure above are representative of actual values, but real vegetation is much more varied (Earthobservatory.nasa.gov, 2017).

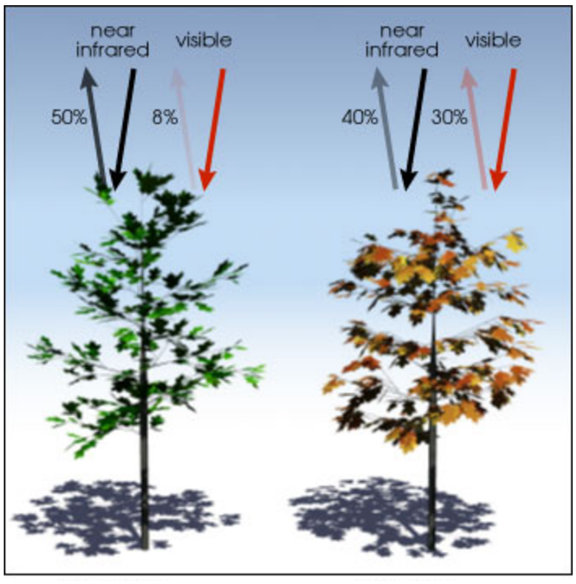

Figure 8. Healthy and Unhealthy vegetations (Earthobservatory.nasa.gov, 2017)

Written mathematically, the formula is:

NDVI = (NIR — VIS)/ (NIR + VIS)

NIR= Near Infrared
VIS= Visible Infrared

The calculations of NDVI for any given pixel, always result in a number that ranges from negative one (-1) to positive one (+1); however, where there are no green leaves present, this value is a closer to zero. While, the number zero signifies a total lack of vegetation; very low values of NDVI (0.1 and below) correspond to barren areas which include areas with relatively large quantities of rocks, sand, or snow. Moderate values represent shrub and grassland (0.2 to 0.3), while high values indicate temperate and tropical rainforests (0.6 to 0.8) (Earthobservatory.nasa.gov, 2017; USGS, 2016).

4. STUDY AREA AND DATA

A multitude of factors within this study area impact the formation of UHI.These include the surrounding ecological biosphere, the total area of the city, the total number of inhabitants residing within the city, the topographic form of the urban landscape, as well as the developmental framework of the city.

4.1 Study Area

Prague is the capital and alpha city of the Czech Republic. The City has an area of 496 km and is located on the banks of the Vltava River on the North-Western centre of the Bohemian Basin (Ucl.ac.uk, 2017).

The City of Prague, just as with other large cities across the globe, must manage to find a happy median between urbanization and maintaining the overall quality of the environment. The heavy impact human beings have on the environment in more developed and industrialized societies is particularly pronounced, as heavy traffic,

pollution, and protracted human habitation have led to the alteration, if not the complete devastation of the pristine pre-settlement state of the environment. Nevertheless, initiatives aiming for the sustainable usage of land, the effective management of waste, as well as water and energy resources, can go a long way in mitigating the negative impact that human habitation has on the natural environment, while restoring some semblance of greenery and natural beauty to the greater urban area. (Prague Environment 2009)

Geography

As it shown in the Fig, the western part of Prague has a higher elevation, while the northeast and southeast parts of Prague also can be attributed to possessing comparatively high degree of elevation. These physical conditions make Prague shape's resemble that of a bowl, which acts in decreasing wind speed, air circulation and contributes to trapping heat within the City. Consequently, city center and surrender have relatively low wind speed.

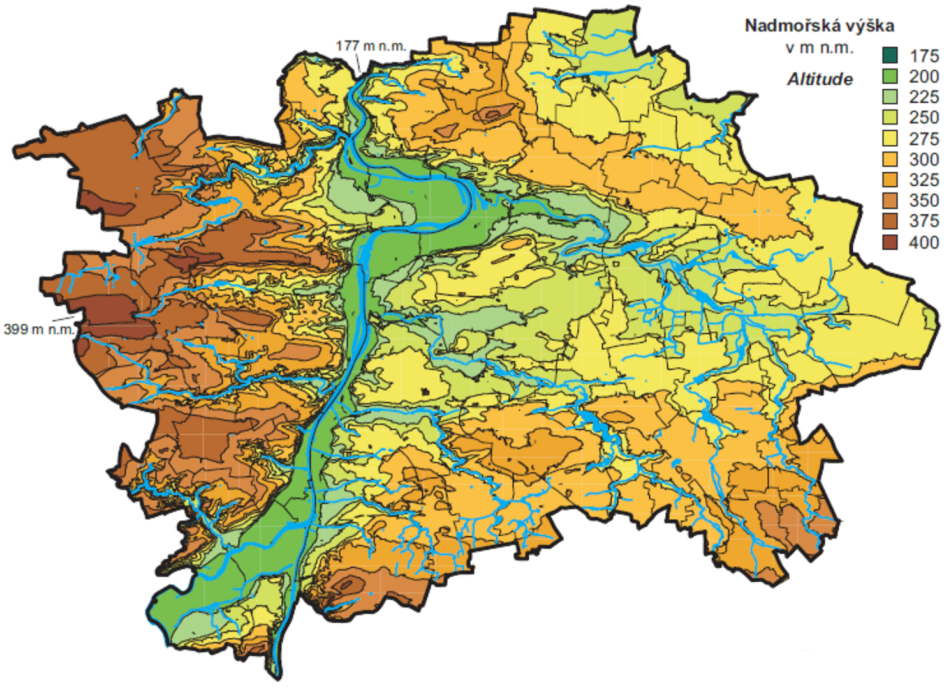

Figure 9. Physical Map of Prague (Source: ÚRM, MHMP)

Population

The population of Prague has gradually increased during the past decades, adding an additional 21,000 inhabitants in 2017 alone, a 1.6 percent net gain for the Greater Prague Area. (Worldpopulationreview.com, 2017)

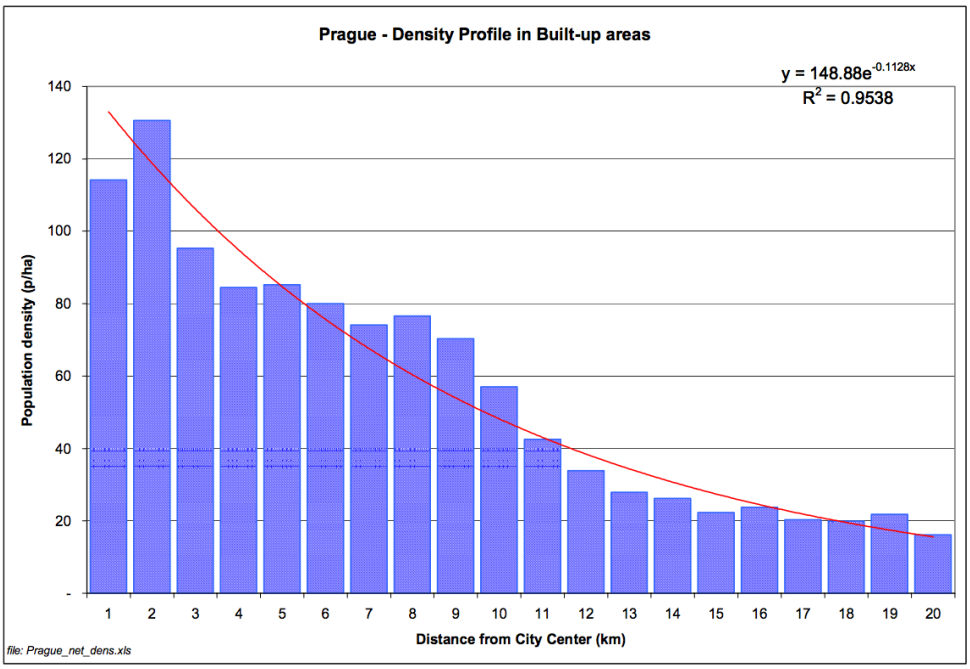

Figure 10. Prague Density Profile in Built-up Areas (Alainbertaud.com, 2017)

As it shown in the figure above: the population is more densely clustered in the city center and the number of inhabitants gradually decreases as the distance from the city center increases.

Climate

Prague, according to Köppen-Geiger ‘s climate classification system, is in humid continental climate (Dfb) zone; the mean temperature of the coldest month below −3 °C and at least four months whose mean temperatures are at or above 10 °C (Peel, Finlayson and McMahon, 2007).

4.2 Selection of Satellite Image

Selecting the correct satellite and imagery is necessary for the remote sensing method. Spatial resolution, spectral resolution, radiometric resolution, temporal resolution are five characteristics to describe each technique.

Since UHI effect can occur in the city center and constructed areas, this study has been conducted within the administrative boundary of Prague, where both built and unbuilt environments are taken into account in identifying the Urban Heat Island effect.

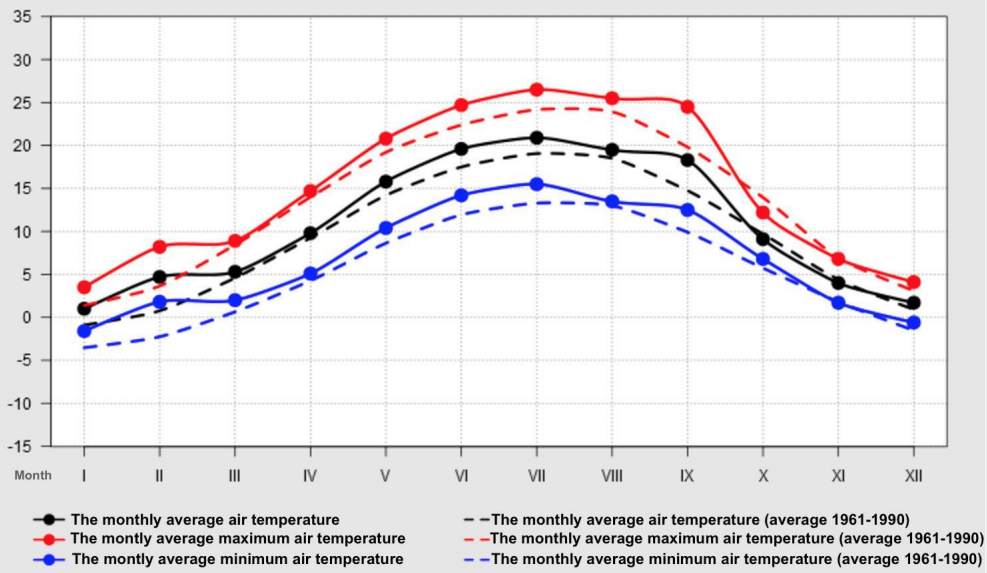

Figure 11. The monthly average distribution, monthly average maximum and minimum air temperatures in comparison with the long-term average 1961-1990 (Portal.chmi.cz., 2017). (Climatological stations Prague-Karlov (260 m), represents urban area)

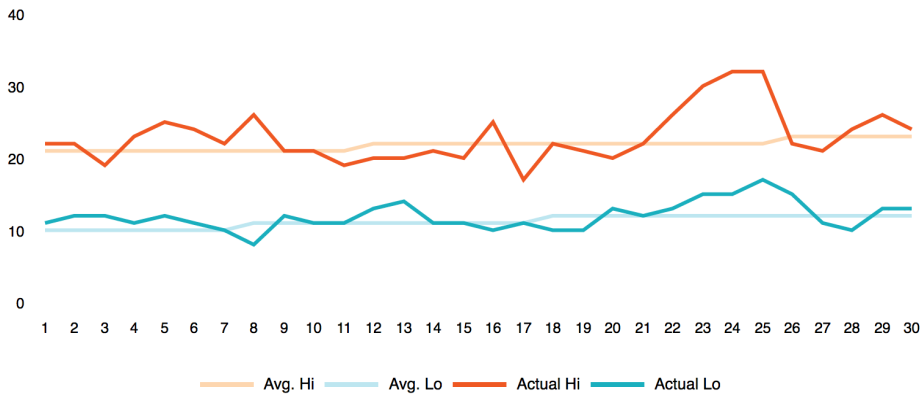

Figure 12. Temperature of June 2016 (AccuWeather, 2017).

Besides the appropriate satellite selection, it is also important to date of the satellite image captured. Due to aim of this study, Analysis of the spatial distribution of Land Surface Temperature (LST) and its relationship with the Normalized Difference Vegetation Index (NDVI), the hottest summer day of June 2016, which had a temperature of approximately 32°C, was selected (AccuWeather, 2017). Because, on that hot summer day the UHI was particularly severe and this consequently provides the optimum conditions to coalesce, in carrying out effective vegetation analysis. The other criteria for optimum satellite image selection is cloud cover; as clouds sometimes cause false interpretations of imagery, which goes onto to impact the quality and accuracy of the image. (Yuksel, 2015)

To derive LST and NDVI over the study area, a Landsat 8 image was used. Selected Landsat 8 OLI TIRS images of path 192, row 25, were acquired from website of the US Geological Survey (USGS) EarthExplorer (http://earthexplorer.usgs.gov/) in GeoTIFF format. The image was captured at approximately 09:56 am (UTM), local time 11:56 (Czech Republic UTM+2) under clear atmospheric conditions (0.4% cloud coverage). On the day the image was captured, the air temperature in Prague was approximately 32°C (AccuWeather, 2017)

Operational Land Imager (OLI) and a Thermal Infrared Sensor (TIRS) sensors are carried by Landsat 8. This thesis employs both sensors in order to investigate the relationship between NDVI and the Land Surface Temperature (LST). A Landsat-8

OLI/TIRS image contains eleven bands, including eight multispectral (Bands 1–7 and 9), one panchromatic (Band 8) and two thermal (Bands 10 and 11) (Estoque et al., 2017) (Fig.13).

Electromagnetic region	Band	Wavelength (μm)	Spatial resolution (m)
Coastal aerosol	1	0.43–0.45	30
Blue	2	0.45–0.51	30
Green	3	0.53–0.59	30
Red	4	0.64–0.67	30
Near infrared (NIR)	5	0.85–0.88	30
Short wave infrared (SWIR) 1	6	1.57–1.65	30
Short wave infrared (SWIR) 2	7	2.11–2.29	30
Panchromatic	8	0.50–0.68	15
Cirrus	9	1.36–1.38	30
Thermal infrared (TIR) 1	10	10.60–11.19	100[a] (30)
Thermal infrared (TIR) 2	11	11.5–12.51	100[a] (30)

[a] TIRS bands are acquired at 100 m resolution, but have been resampled to 30 m in the delivered data product. Source: http://landsat.usgs.gov.

Figure 13. Features of a Landsat-8 OLI/TIRS image (Estoque et al., 2017)

5. METHODOLOGY

The overall methodology of this thesis is briefly presented below:

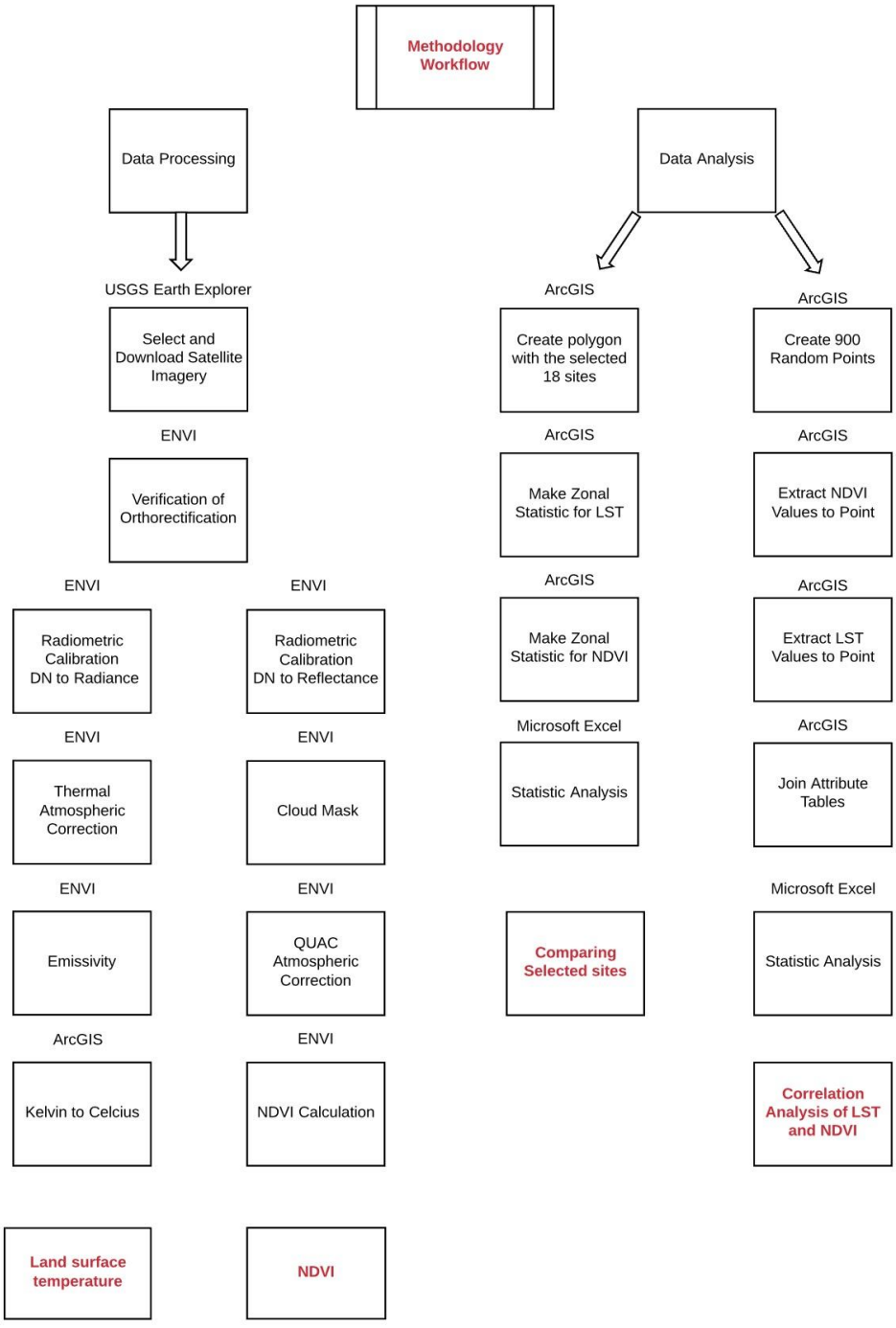

Figure 14. Workflow of the methodology

Satellite data preprocessing has been performed using ENVI 5.3 Software. After the initial step of pre-processing, the satellite images were then used to retrieve LST and

NDVI for analysis of urban heat island in Prague. Further processes have been performed using both ENVI 5.3 and ArcGIS 10.2.1 Software. Statistical analysis was performed using Microsoft Excel Software.

5.1 Satellite Image Processing

All image processing was performed using with ENVI (Environment for Visualizing Images) and ArcGIS Software.

5.1.1 Determination of Land Surface Temperature

5.1.1.1. Conversion of Digital Numbers (DN) to radiance

Before applying the thermal atmospheric correction, raw Landsat dataset needs to be converted to Digital Number (DN) values (for Landsat 8 it is 0-4095, which describe pixel values that have not yet been calibrated into physically meaningful units, to thermal bands (Bands 10 and 11) first to absolute radiance values (USGS,2016, Harris Geospatial Solutions, 2017)

With ENVI software has a radiometric correction option under the Radiometric calibration; which convert DN value to Radiance with the following formula (2)

$L_\lambda = Gain * Pixel\ value + Offset$ (2) (Harrisgeospatial.com, 2017)

L_λ = Radiance in units of W/(m2 * sr * μm)

Gain and offset value are retrieved from the metadata (MTL)

In the Radiometric calibration tool, calibration type was selected as a radiance. Gain and offset values should be retrieved from the image's metadata ın this case, in order to achieve a radiance which represents the sum of radiation coming from an area. It is important to select the right metadata, in this case Landsat 8 thermal metadata (MTL) was selected. For calculation Radiance in units of W/ (m2 * sr * μm), both of the Offset and gain values have to be W/ (m2 * sr * μm) (Harris Geospatial Solutions, 2017)

5.1.1.2. Atmospheric Correction

The radiance values of the satellite imagery contain brightness owing to reflectance of the target of interest; the rest is derived from the atmosphere, which carries no information about the target of interest. (Hadjimitsis et al., 2010)
Therefore atmospheric correction requires the removal of the scattering and absorption effects of the atmosphere from the radiance data for accuracy of subsequent analysis (GIS Geography, 2017).

From the Toolbox, subcategory of Radiometric Correction, Thermal Atmospheric Correction was used with standard settings of the module to atmospheric correction of thermal bands within ENVI software.

5.1.1.3. Converted to Emissivity and Temperature

Emissivity reference channel method was used in order to retrieve LST within ENVI software. This technique supposes that all the pixels in one band have a stationary emissivity. A temperature image is calculated with that stationary emissivity value and using the Planck function, temperatures values applied to calculate the emissivity values in all the other bands. (Harrisgeospatial.com, 2017)

After spatial and spectral subletting were arranged, thermal infrared band 1 (10.900) was selected to be set to a constant emissivity value. As it is not possible to acquire the real emissivity values of all the urban surface. According to the table (Yang et al., 2015), emissivity value was approximated at 0.9600, with the consideration of urban structure density consisting of asphalt concrete and used as Assumed Emissivity Value. Eventually, with the Output Temperature Image option, the temperature image was obtained as a Kelvin unit.

Class	Class-ID	Emissivity in band 10	Emissivity in band 11
Asphalt	A001	0.962	0.960
	A002	0.952	0.965
	A003	0.951	0.959
	A004	0.953	0.966
	A005	0.943	0.960
	A006	0.929	0.955
	A007	0.944	0.965
	A008	0.942	0.965
	A009	0.949	0.958
	A010	0.955	0.965
	Average	0.948	0.962
Cement/concrete	C001	0.947	0.949
	C002	0.945	0.957
	C003	0.938	0.942
	C004	0.956	0.966
	C005	0.958	0.945
	C006	0.953	0.951
	C008	0.956	0.968
	Average	0.950	0.954
Brick	B001	0.965	0.966
	B002	0.951	0.965
	B003	0.944	0.956
	B004	0.911	0.947
	B005	0.960	0.965
	B006	0.930	0.953
	B007	0.961	0.966
	B008	0.938	0.968
	B009	0.956	0.967
	B010	0.936	0.940
	B011	0.961	0.969
	B012	0.952	0.964
	B013	0.956	0.965
	B014	0.962	0.967
	Average	0.949	0.961
Grassland		0.983	0.989
Tree		0.973	0.973

Figure 15. Material Emissivity values in Urban Areas. Source: (Yang et al., 2015)

5.1.1.4. Convert Kelvin to Celsius

In ArcGIS, the Raster calculator tool was used to convert Kelvin temperature to Celsius temperature, which is the official unit of temperature in Europe, with following equation:

$$T(°C) = T(K) - 273.15$$

5.1.2. Normalized Difference Vegetation Index (NDVI)

5.1.1.1. Radiometric Calibration

Digital Number (DN) values have to be calibrated to reflectance, in order to get the most reliable NDVI. From the radiometric calibration dialog, Multispectral metadata file was selected as a select input file and 7 multispectral bands of Landsat 8 OLI was selected with full extent spatial subset (Harris Geospatial Solutions, 2017)

5.1.1.2. Create a Cloud Mask for Landsat

Before attempting the Quick Atmospheric Correction (QUAC) method, clouds have to be masked in order to prevent any false telemetry provided by clouds. From the Toolbox, the subcategory of Feature Extraction, Calculate Cloud Mask using F-mask Algorithm was performed and a new layer where the cloud (masked) pixels have values of 0 and the non-cloud (non-masked) pixels have values of 1, was created. Eventually with the mask option, the new layer was selected as a cloud mask Raster and masked image was created (Harris Geospatial Solutions, 2017).

5.1.1.3. Atmospheric Correction

Prior to NDVI analysis, QUick Atmospheric Correction (QUAC) method, which works with the visible and near-infrared through shortwave infrared (VNIR-SWIR) wavelength range, was used in order to apply atmospheric corrections. (Harrisgeospatial.com, 2017). Furthermore, QUAC has notably faster computational speed compared to other physics-based, first-principle methods (FLAASH). Since Landsat 8 OLI multispectral image have seven bands, Sensor-type was selected as Near-Shortwave Infrared (NIR-SWIR) (Harrisgeospatial.com, 2017).

5.1.1.4. NDVI calculation

From the Spectral Indices tool, NDVI (Normalized Difference Vegetation Index) which is a part of the vegetation index, was used in order to transform multispectral data into a single image band indicating vegetation distribution.
NDVI is calculated from these individual measurements as follows:

$$\text{NDVI} = \frac{NIR - Red}{NIR + Red}$$

Before the calculation, it has to be considered that NIR (Near infrared) and red band varies depending on the satellite. Since Landsat 8 OLI image was used in this study, red band 4 (0.64-0.67 µm) and NIR band 5 (0.85-0.88 µm) were set as an NDVI calculation parameters. (Harris Geospatial Solutions, 2017)

$$\text{NDVI} = \frac{band\ OLI5 - band\ OLI4}{band\ OLI5 + band\ OLI4}$$

5.2 DATA ANALYSIS

5.2.1 Relationship between NDVI and LST

In order to examine the relationship between NDVI and LST, with the "Create Random Point" operator, 900 points were created with ArcGIS software. So as to obtain any meaningful result, the distance between two pixels was determined to be 200m, in order to avoid two points having the same pixel value. 6 points were extracted which are represented in order to prevent the presence of water from complicating things with incorrect data. The Extract values to point operator was performed with both NDVI and LST imagery with the remaining 894 points. From this attribute table, these two datasets were adjoined. The joined attribute table was extracted to Excel, and correlation analysis was performed.

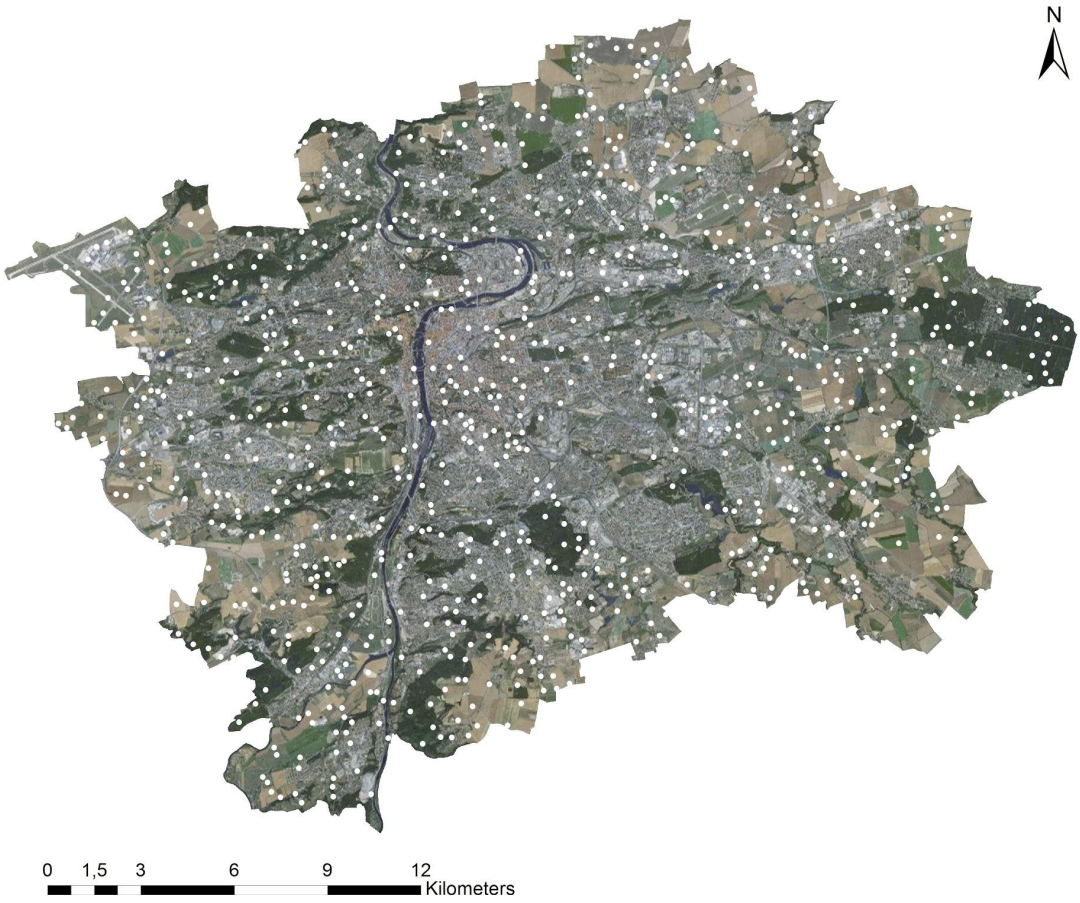

Figure 16. Spatial distribution of the dispersed 894 points in study area

5.2.2. Selected Sites

In order to investigate how the UHI effect is expressed in different areas and its relationship with LST and NDVI, eighteen different sites were selected due to several key similarities and differences such as a park, an industrial area, as well as a green residential area. The eighteen selected sites were presented in the map (Fig.17).

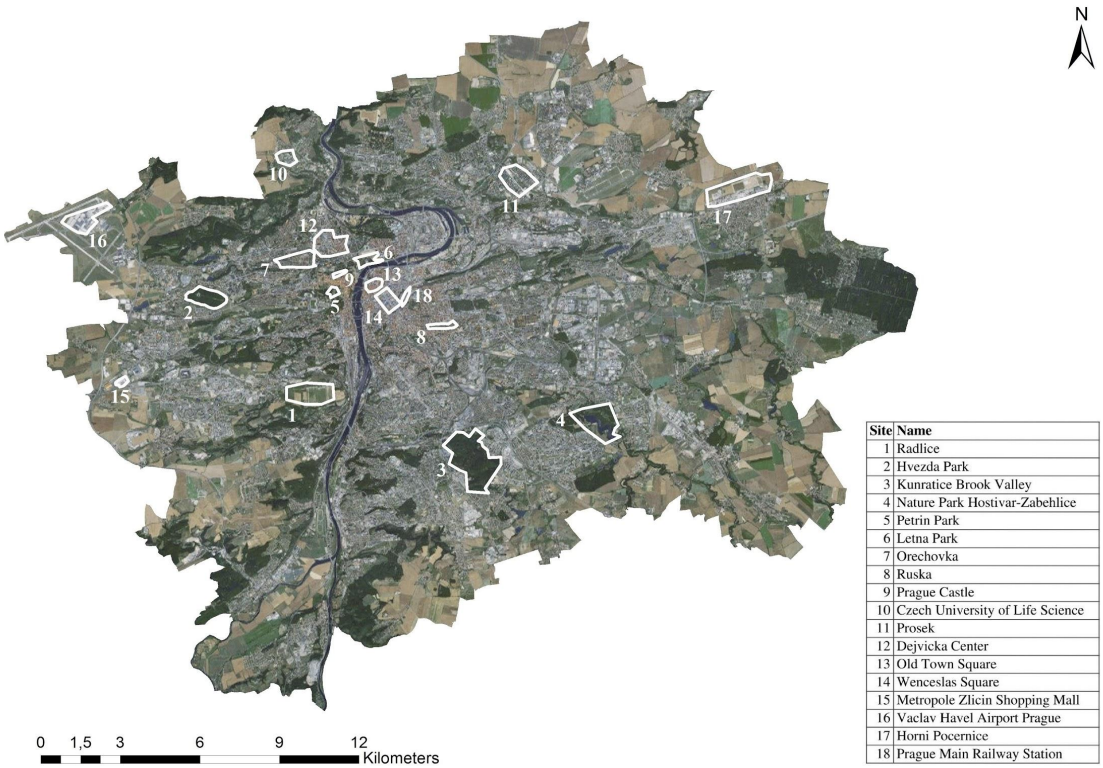

Figure 17. The 18 selected sites of this thesis presented in the map.

Table 1. Description of the 18 selected sites

Site	Name	Description
1	Radlice	Agriculture
2	Hvezda Park	Park
3	Kunratice Brook Valley	Urban Forest
4	Nature Park Hostivar-Zabehlice	Nature Park
5	Petrin Park	Park
6	Letna Park	Park
7	Orechovka	Green residential
8	Ruska	Green residential
9	Prague Castle	Castle
10	Czech University of Life Science	University Campus
11	Prosek	Prefabric Residential
12	Dejvicka Center	Tentment buildings
13	Old Town Square	Tentment buildings
14	Wenceslas Square	Tentment buildings
15	Metropole Zlicin Shopping Mall	Commercial
16	Vaclav Havel Airport Prague	Airport
17	Horni Pocernice	Industrial Area
18	Prague Main Railway Station	Railway station

6. RESULTS

The city center features prominently in the LST image, due to a sharp contrast between high and low LSTs within the city center (Fig.18). Nevertheless, relatively low LSTs could also be observed within the central part of the Prague due to the numerous small parks distributed around the city. The adjacent vicinity of City Centre (Prague 1) is known as the Heart of Prague, due to its collection of main city services and tourist attractions. Consequently, this area has a high population density and built-up area. The lowest LST observed was in the very southeast part of the city, comprised of a vast agricultural area and several nature parks.

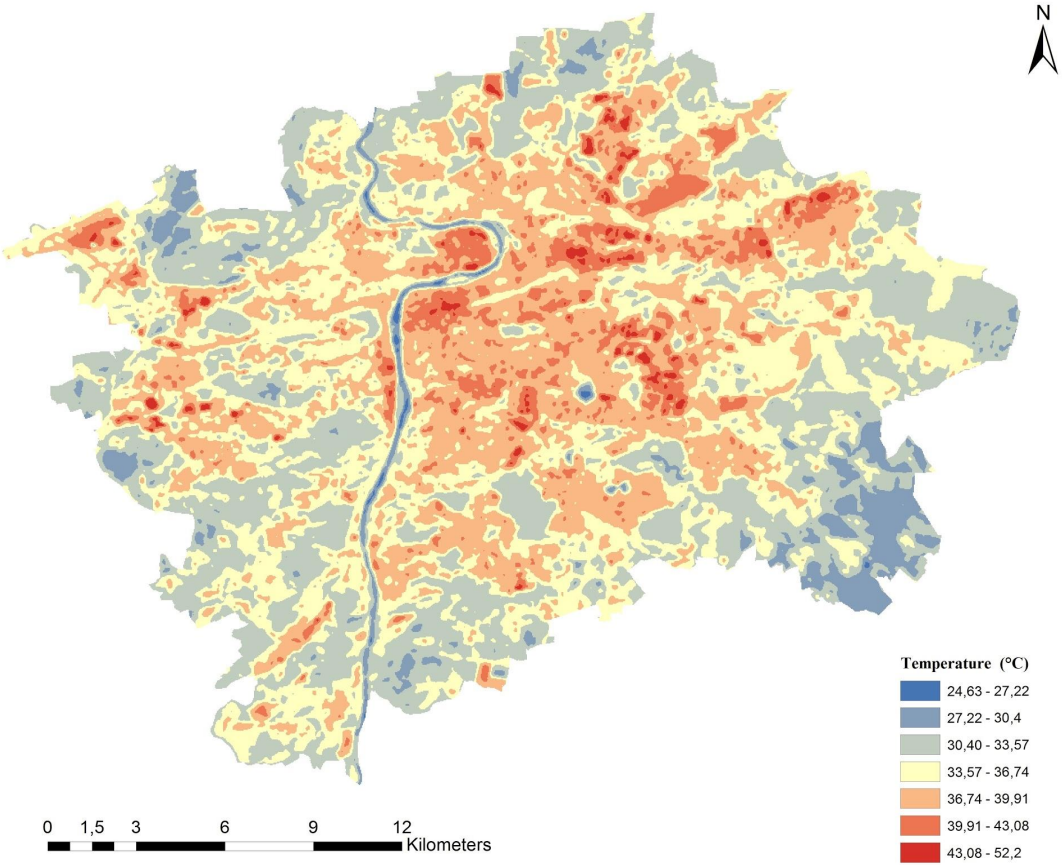

Figure 18. Distribution of land surface temperature in Prague on 24th June 2016 derived from Landsat 8 image

It is known that water bodies lower the LST of the surrounding area through ventilated corridor and water evaporation processes. This fact can be clearly seen in

Fig. 18. However, due to the built-up areas, which are very close to the Vltava River, this ventilated corridor does not reach to the interior portion of the city.

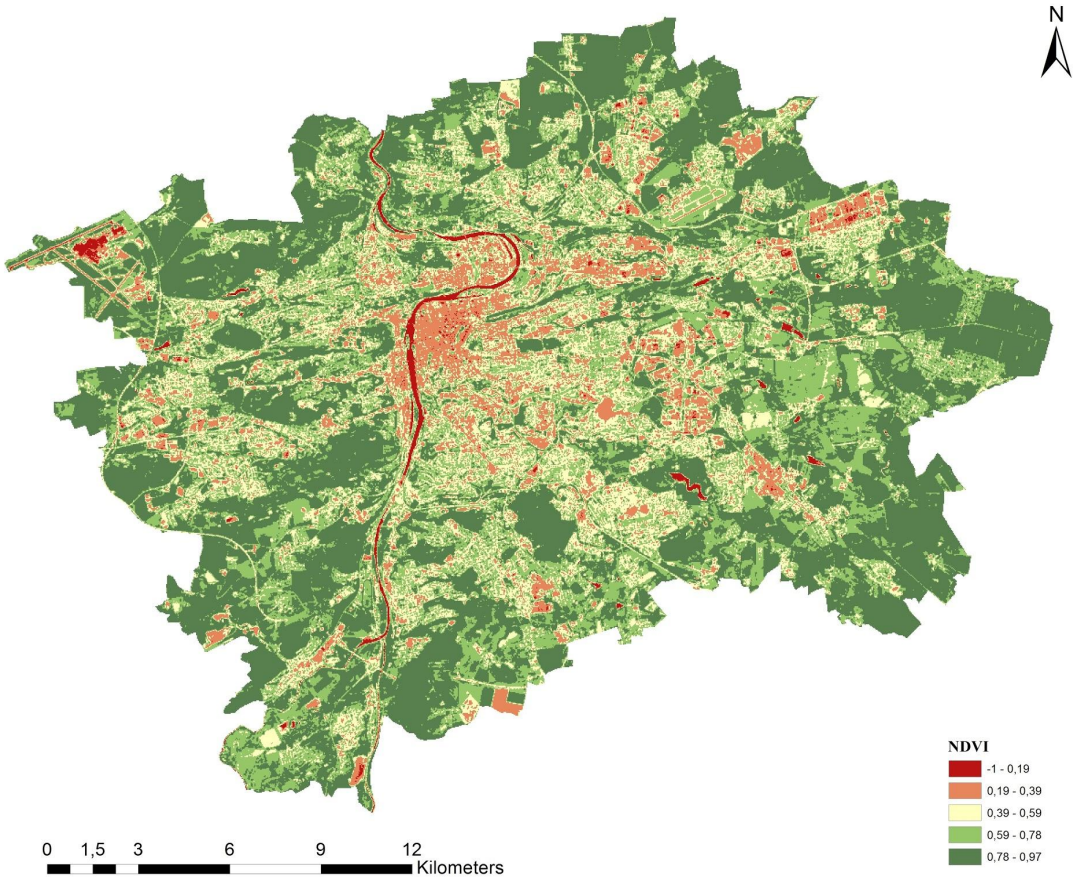

Figure 19. Distribution of NDVI in Prague on 24th June 2016 derived from Landsat 8 image

Distribution of NDVI map (Fig) showed that, the areas having a low value of NDVI have a direct correlation with areas that are highly built up i.e. in the city center (Prague 1). On the other hand, high NDVI value was found mostly in the outer portions of the city and the open areas.

As a result, the high levels of NDVI exist dispersed around the boundary of the city, especially in southwest sector, the Natural Park Radotínsko-Chuchelský háj (Grove).

Site	Name	Temperature (°C)	NDVI
1	Radlice	31,13	0,85
2	Hvezda Park	31,2	0,92
3	Kunratice Brook Valley	31,88	0,9
4	Nature Park Hostivar-Zabehlice	32,09	0,73
5	Petrin Park	32,9	0,86
6	Letna Park	35,52	0,77
7	Orechovka	35,99	0,66
8	Ruska	37,26	0,64
9	Prague Castle	37,4	0,33
10	Czech University of Life Science	37,51	0,59
11	Prosek	37,84	0,61
12	Dejvicka Center	38,22	0,44
13	Old Town Square	40,02	0,3
14	Wenceslas Square	40,39	0,29
15	Metropole Zlicin Shopping Mall	40,58	0,31
16	Vaclav Havel Airport Prague	40,79	0,25
17	Horni Pocernice	40,93	0,34
18	Prague Main Railway Station	40,97	0,22

Figure 20. LST and NDVI values for selected sites

The results of LST and NDVI values for selected sites are given in Table 2.
The table shows that agricultural area (Radlice) has the lowest LST (31.2°C) with high NDVI value (0.85) followed by greenery areas (Hvezda 31.2°C), Kunratice Brook Valley (31.88 °C), Nature Park Hostivar Zabehlice (32.09°C) and Petrin Park (32.09°C), as would be expected. The highest LST Is founded at Prague Main Railway Station (40,97°C) followed by Industrial area (Horni Pocernice) with (40.93°C) and 0.34 NDVI, Vaclav Havel Airport (40.79°C) and 0.25 NDVI, Metropole Zlicin Shopping Mall (40,58°C), Wenceslas Square (40.39°C), and Old Town Square (40.02°C).

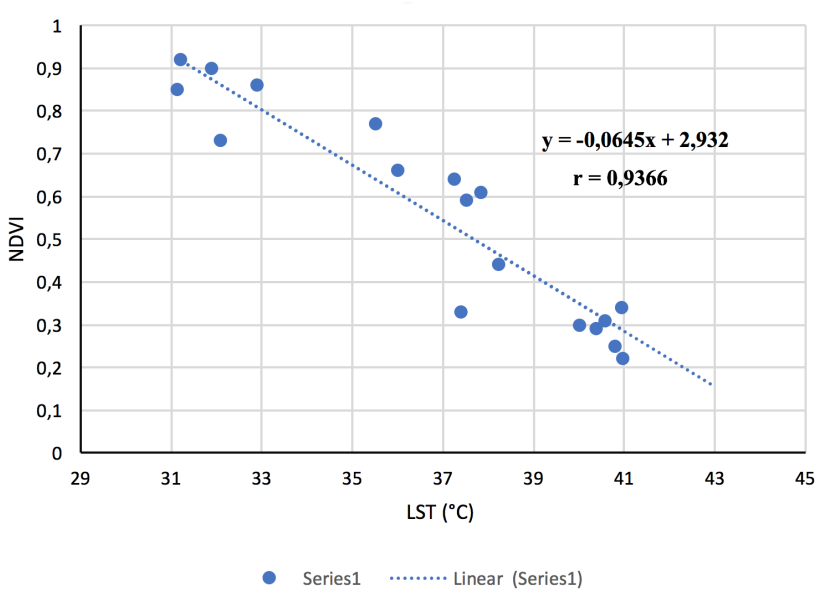

Figure 21. LST and NDVI relationship of the selected sites

As it is recognizable from the table and figure, the relationship between LST and NDVI show a strong inverse relationship (r=-0,9366). Some unexpected results were found in selected sites. Even though Letna park has 0.77 NDVI value like Kunratice Brook Valley 0.73, surprisingly, its temperature is 3.64 °C higher than Kunratice Brook Valley. This temperature is closer to the Orechovka green residential site with (35.99°C).

Another surprising result is Prague Castle, which has temperature (37.4°C) and 0.33 NDVI value. Despite its low NDVI value, it has a similar temperature with green residential areas.

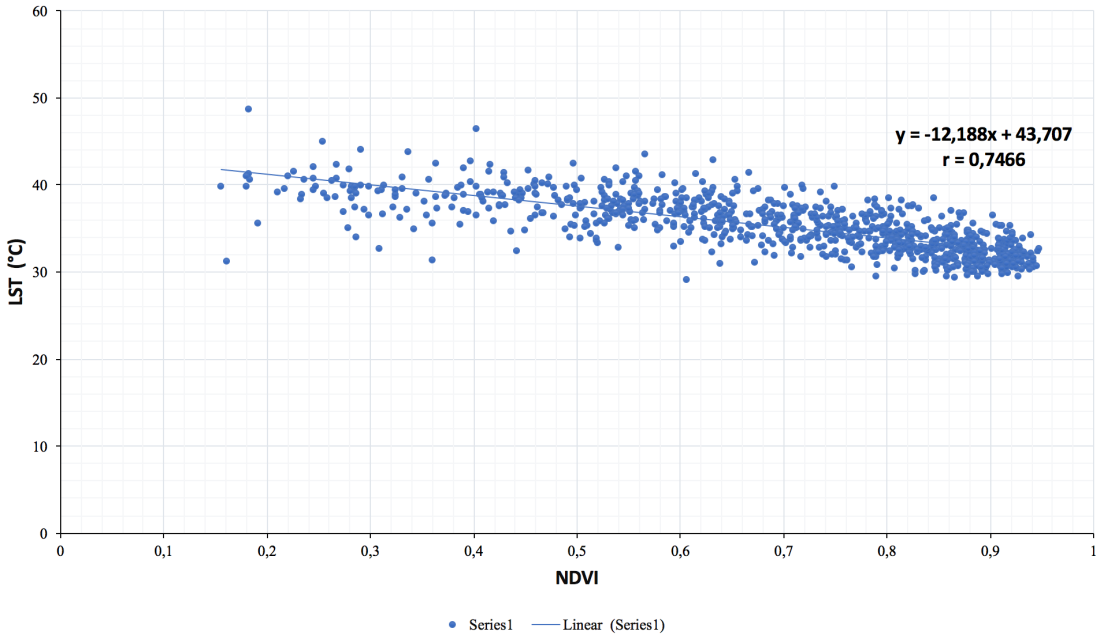

Figure 22. LST and the NDVI relationship

As is shown in the Fig. 22, the results indicated a strong inverse relationship (r =-0.74) between LST and the NDVI. When NDVI is high, the LST is low. Two areas with opposite temperature can be observed. The highest temperature was observed in the O2 Arena with (48.71 °C) and 0.12 NDVI value. The lowest temperature was observed in the agricultural area which is located in southeast Prague with (29.30 °C) and 0,61 NDVI value.

7. DISCUSSION

The aim of this dissertation was determining and evaluating the effects that UHI has on Prague by using a remote sensing approach. Analysis will be given on the spatial distribution of Land Surface Temperature (LST) and its relationship with Vegetation density calculated by an index known as Normalized Difference Vegetation Index (NDVI) using thermal remote sensing data. Both ENVI 5.3 and ArcGIS 10.2.1

Results showed that the spatial distribution of the land surface temperature was affected by the NDVI. Comparing the NDVI and LST maps, the areas with dense built-up and less vegetation cover, which cause a reduction in the evaporative and cooling qualities of shadows, which indicate a comparatively higher surface temperature. On the contrary, areas covered by vegetation and water bodies were indicated comparatively lower surface temperature.

Between two warmer and colder values, there are also similar areas which have an average temperature and NDVI values. It represents mostly the green residential area where vegetation cover and built-up area coexist. Urban areas with low vegetative cover are more vulnerable to the UHI effect in Prague.

Results of the maps and analysis showed that some areas which has low vegetation cover and high built up density, impacted by UHI. Consequently, these results showed the significant effectiveness of the vegetation cover in terms of mitigation UHI.

As it is recognizable from the table and figure, the relationship between LST and NDVI show a strong inverse relationship (r=-0,9366). Unexpectedly, some results were contradictory to the NDVI and LST correlation. Even though Letna park has 0.77 NDVI value, its temperature is 3.64 °C higher than other green areas with similar NDVI value. On the contrary Prague Castle has cooler temperature than other areas which has similar NDVI value. The most likely explanation of the negative finding is the other factors which effect the LST such as elevation, slope aspect, topography and so forth.

The main limitation of this study is that while examining the relationship between NDVI and LST, does not include parameters for the other factors which also affect LST, such as topography of location, local wind direction and speed, slope aspect. Even though most of the results followed the correlation between NDVI and LST, as it explains above some results showed that necessity for the including other parameters.

Although this study was conducted in Prague, the results for strong inverse NDVI and LST relationship generalizable to other areas.

Mitigation Strategies for UHI

Akbari and Kolokotsa (2016) described two fundamental strategies: the first of which encompasses the rise in solar reflectance in order to decrease the total solar radiation in urban elements. The second being able to maximize the vegetation cover in order to increase evapotranspiration.

For the new plan of the urban area it is important to consider physical properties in order to mitigate UHI effect:(Giridharan, 2004)
- Urban structure (spatial distrubition of urban area)
- Size of the city (population, density of built-up area)
- Ratio of building height to distance between each other
- Width of the streets
- Building materials (albedo, heat capacity)
- Surface materials (asphalt, concrete)
- Sky-view factor (Giridharan, 2004)

Thus, in order mitigate the UHI effect in a planned city such as Prague, cool roof (green roof and white roof), cool pavements, urban trees are possible mitigation solutions.

In our findings also shows that green residential areas cooler than built up areas. Furthermore, Researchers (Lensky et al., 2015) founded that private residential garden could be more efficiently used for vegetation cover, than the small to medium public park space found throughout Tel Aviv. Just as with the green roof, increasing garden distance between two building and encouraging private gardens would also be recommended.

For the selection of mitigation strategy; both historical and characteristic values of the area should also be considered. In this thesis. Old Town Square was founded in UHI affected area with high LST (40.02°C)) and low NDVI value (0.3). Even white roofs are very effective in mitigating UHI. However, given the aesthetic and historical value of the Old Town Square, it simply isn't an option in this specific locale. However, this option is suitable for the newly built up areas such as the Metropole Zlicin Shopping Center or the industrial site of Horni Pocernice.

Decision makers and planners have an important role in deciding as to whether adopting a mitigation strategy is needed or which strategy in general should be implemented. Hence, they need to understand the terms of UHI, the specific characteristics, and spatial distributions in the area.

For instance, Municipality of Samsun mandates to contractors who make the new buildings, to plant new tree related to number of apartments. The key point is the location of the new trees, where they proposed, outside of the City. Even Though they implement the increasing greenery mitigation strategy, the missing point is not created spatial distribution of the UHI and not detect the heat vulnerable zones. On the other hand, planting new tree is beneficial in terms of environment but, Since the municipality offer place for planting outside the city where does not vulnerable to UHI, it doesn’t serve the real intention of project which says, “green municipality”. On the contrary to that, new law of France, which mandates that all new buildings that are built in commercial zones must be partially covered in either plants or solar panels, would be more efficient in terms of the UHI, because commercial zones are more vulnerable to heat extreme.

Further studies are required to establish other parameters such as NDBI (the normalized difference built-up index), in order to examine its relationship with NDVI and LST.

8. CONCLUSION

In this study, LST and NDVI were retrieved by using the Landsat 8 OLI/TIRS data. By assessing the findings retrieved from LST and NDVI, it is found that the distribution of urban heat islands in Prague is mainly concentrated in city center and surrounding areas.

The result of this thesis, observed through the comparing the spatial distribution of NDVI and LST maps, clearly illustrate the LST was affected by the vegetation cover in Prague. Moreover, the correlation analysis between LST and NDVI also verified the strong inverse relationship (r =-0,74). Both of the results from spatial distribution maps and statistical analysis are proved the hypothesis of the thesis premise which refers land surface temperature can gradually increase in Prague due to urban growth and decreasing greenery.

The results of this thesis endorse other findings in several study areas conducted across the world: thereby highlighting the necessity of considering vegetation cover in city planning as an effective means of mitigating UHI´s effects.

In terms of the mitigation strategies of UHI, it is of particular importance to take into account the effectiveness of strategies. In order to accomplish this, a land surface temperature map of the city should be used, critical heat zones should be identified, and strategies should be implemented according to the information available, and with respect to the various individual characteristics of each respective city.

The results of this study can be effectively corroborated with further analysis of UHI related factors. Furthermore, both urban planners and decision makers can reference this study in order assess the mitigation measures throughout Prague.

9. REFERENCES

AccuWeather. (2017). Prague June Weather 2016 - AccuWeather Forecast for Prague Czech Republic. [online] Available at: http://www.accuweather.com/en/cz/prague/125594/june-weather/125594?monyr=6/1/2016&view=table [Accessed 10 Mar. 2017].

Alainbertaud.com. (2017). Alain Bertaud | The study of urban spatial structures. [online] Available at: http://alainbertaud.com/ [Accessed 18 Mar. 2017].

Alonso, M.S., Labajo, J.L., & Fidalgo, M.R. (2003). Characteristics of the urban heat island in the city of Salamanca, Spain. Atmósfera, 16(3), 137-148.

Argaud, L., Ferry, T., Le, Q.-H., Marfisi, A., Ciorba, D., Achache, P., Ducluzeau, R., Robert, D. (2007). Short- and long-term outcomes of heatstroke following the 2003 heat wave in Lyon, France. Archives of Internal Medicine, 167(20), 2177–2183.

Arnfield, A.J. (2003) 'Two decades of urban climate research: A review of turbulence, exchanges of energy and water, and the urban heat island', International Journal of Climatology, 23(1), pp. 1–26. doi: 10.1002/joc.859.

Bokaie, M., Zarkesh, M., Arasteh, P. and Hosseini, A. (2016). Assessment of Urban Heat Island based on the relationship between land surface temperature and Land Use/ Land Cover in Tehran. Sustainable Cities and Society, 23, pp.94-104.

Byles, J. (2017). How to beat extreme heat: Strategies for combating the urban heat island effect — Broken Sidewalk. [online] Broken Sidewalk. Available at: https://brokensidewalk.com/2016/urban-heat-island-effect/ [Accessed 24 Mar. 2017].

C2es.org. (2017). Extreme Heat and Climate Change | Center for Climate and Energy Solutions. [online] Available at: https://www.c2es.org/science-impacts/extreme-weather/extreme-heat [Accessed 18 Feb. 2017].

Ca, V. T., Asaeda, T., & Abu, E. M. (1998). Reductions in air conditioning energy caused by a nearby park. Energy and Buildings, 29(1), 83–92.

Che-Ani, A.I., Shahmohamadi, P., Sairi, A., Mohd-Nor, M.F.I., Zain, M.F.M., & Surat, M. (2009). Mitigating the urban island effect: some points with altering existing city planning. European Journal of Scientific Research, 35(2), 204-216.

Chen, X., Zhao, H., Li, P. and Yin, Z. (2006). Remote sensing image-based analysis of the relationship between urban heat island and land use/cover changes. Remote Sensing of Environment, 104(2), pp.133-146.

Climate.ncsu.edu. (2017). Earth's Energy Balance | Climate Education Modules for K-12. [online] Available at: http://climate.ncsu.edu/edu/k12/.eeb [Accessed 26 Feb. 2017].

Cochran, N.E. (2014) Detection of urban heat islands in the great lakes region with GLOBE student surface temperature measurements. MSC thesis.

Crisp.nus.edu.sg. (2017). Principles of Remote Sensing - Centre for Remote Imaging, Sensing and Processing, CRISP. [online] Available at: http://www.crisp.nus.edu.sg/~research/tutorial/infrared.htm [Accessed 9 Jan. 2017].

Dixon, P. G., & Mote, T. L. (2003). Patterns and Causes of Atlanta's Urban Heat Island–Initiated Precipitation. Journal of Applied Meteorology, 42(9), 1273–1284.

Díaz, S., Hector, A., & Wardle, D. a. (2009). Biodiversity in forest carbon sequestration initiatives: not just a side benefit. Current Opinion in Environmental Sustainability, 1(1), 55–60.

Duman, Ü. and Juyal, M. (2004) Climate, Design and Sustainable Cities. XXXII IAHS World Congress on Housing Sustainability of the Housing Projects - September 21-25, 2004, Trento, Italy

EPA (US Environmental Protection Agency), (2008) Reducing Urban Heat Islands: Com- pendium of Strategies. US Environmental Protection Agency, Washington, D.C.

Epa.gov. (2017). Measuring Heat Islands | Heat Island Effect | US EPA. [online] Available at: https://www.epa.gov/heat-islands/measuring-heat-islands#main-content) [Accessed 9 Mar. 2017].

Esseacourses.strategies.org. (2017). Institute for Global Environmental Strategies >> Global Climate Change: Albedo. [online] Available at: http://esseacourses.strategies.org/module.php?module_id=99 [Accessed 24 Mar. 2017].

Estoque, R., Murayama, Y. and Myint, S. (2017). Effects of landscape composition and pattern on land surface temperature: An urban heat island study in the megacities of Southeast Asia. Science of The Total Environment, 577, pp.349-359.

Finkenbine, J. K., Atwater, J. W., & Mavinic, D. S. (2000). Stream health after urbanisation. Journal of the American Water Resources Association, 36(5), 1149–1160.

Fouillet, a., Rey, G., Laurent, F., Pavillon, G., Bellec, S., Guihenneuc-Jouyaux, C., Hémon, D. (2006). Excess mortality related to the August 2003 heat wave in France. International Archives of Occupational and Environmental Health, 80(1), 16–24.

Gedzelman, S.D., Austin, S., Cermak, R., Stefano, N., Partridge, S., Quesenberry, S., and Robinson, D.A., (2003): Mesoscale aspects of the urban heat island around New York City. Theoretical Applied Climatology, 75(1–2), 29–42.

GIS Geography. (2017). What is Atmospheric Correction in Remote Sensing? - GIS Geography. [online] Available at: http://gisgeography.com/atmospheric-correction/ [Accessed 8 Mar. 2017].

Hadjimitsis, D., Papadavid, G., Agapiou, A., Themistocleous, K., Hadjimitsis, M., Retalis, A., Michaelides, S., Chrysoulakis, N., Toulios, L. and Clayton, C. (2010). Atmospheric correction for satellite remotely sensed data intended for agricultural applications: impact on vegetation indices. Natural Hazards and Earth System Science, 10(1), pp.89-95.

Harris Geospatial Solutions. (2017). Digital Number, Radiance, and Reflectance. [online] Available at: http://www.harrisgeospatial.com/Home/NewsUpdates/TabId/170/ArtMID/735/ArticleID/13592/Digital-Number-Radiance-and-Reflectance.aspx [Accessed 1 Mar. 2017].

Harrisgeospatial.com. (2017). Atmospheric Correction (Using ENVI) [Harris Geospatial Docs Center]. [online] Available at: http://www.harrisgeospatial.com/docs/AtmosphericCorrection.html [Accessed 9 Mar. 2017].

HowStuffWorks. (2017). How Thermal Imaging Works. [online] Available at: http://electronics.howstuffworks.com/thermal-imaging1.htm [Accessed 8 Feb. 2017].

Jones, H. G. & Vaughan, R. A. (2010). Remote sensing of vegetation: Principles, techniques, and applications. Oxford University Press, Oxford, New York.

Kikon, N., Singh, P., Singh, S. and Vyas, A. (2016). Assessment of urban heat islands (UHI) of Noida City, India using multi-temporal satellite data. Sustainable Cities and Society, 22, pp.19-28.

Koppe, C., Kovats, S., Jendritzky, G., Menne, B. and Breuer, D. (2004). Heat waves. 1st ed. Copenhagen: Regional Office for Europe, World Health Organization.

Krause, C. W., Lockard, B., Newcomb, T. J., Kibler, D., Lohani, V., & Orth, D. J. (2004). Predicting influences of urban development on thermal habitat in a warm water stream. Journal of The American Water Resources Association, 40(6), 1645–1658.

Kusaka, H., Kimura, F., Hirakuchi, H., & Mizutori, M. (2000). The Effects of Land-Use Alteration on the Sea Breeze and Daytime Heat Island in the Tokyo Metropolitan Area. Journat of the Meteorotogical Society of Japan, 78(4), 405–420.

Landsat.gsfc.nasa.gov. (2017). Where to Get Data « Landsat Science. [online] Available at: https://landsat.gsfc.nasa.gov/data/where-to-get-data/ [Accessed 6 Feb. 2017].

Landsat.usgs.gov. (2017). Landsat 8 (L8) Data Users Handbook | Landsat Missions. [online] Available at: https://landsat.usgs.gov/landsat-8-l8-data-users-handbook [Accessed 5 Mar. 2017].

Landsberg, H.E. (1981) The urban climate. Academic Press.

Luber, G. and McGeehin, M. (2008). Climate Change and Extreme Heat Events. American Journal of Preventive Medicine, 35(5), pp.429-435.

Mirzaei, P.A. and Haghighat, F. (2010) 'Approaches to study urban heat island – abilities and limitations', Building and Environment, 45(10), pp. 2192–2201. doi: 10.1016/j.buildenv.2010.04.001.

Nunez, M., & Oke, T. R. (1976). Long-wave radiativeflux divergence and nocturnal cooling of the urban atmosphere—II. Within an urban can- yon. Boundary-Layer Meteorology, 10, 121–135.

Oke, T. R. (1982). The energetic basis of the urban heat island. Q. J. R. Meteorol. Soc. 108, 1–24.

Oke, T. R. (1987). Boundary Layer Climates. London: Routledge.

Oke, T. R. (1995). The heat island of the urban boundary layer: Character- istics, causes and effects. In J. E. Cermak, A. G. Davenport, E. J. Plate, & D. X. Viegas (Eds.), Wind climate in cities (pp. 81–107). Dordrecht: Kluwer Academic.

Payton, S., Lindsey, G., Wilson, J., Ottensmann, J. R., & Man, J. (2008). Valuing the benefits of the urban forest: a spatial hedonic approach. Journal of Environmental Planning and Management, 51(6), 717–736.

Peel, M., Finlayson, B. and McMahon, T. (2007). Updated world map of the Köppen-Geiger climate classification. Hydrology and Earth System Sciences, 11(5), pp.1633-1644.

Portal.chmi.cz. (2017). Portál ČHMÚ: Historická data : Počasí : Měsíční data. [online] Available at: http://portal.chmi.cz/historicka-data/pocasi/mesicni-data# [Accessed 3 Mar. 2017].

R. Giridharan, S. Ganesan, S.S.Y. Lau (2004) : "Daytime urban heat island effect in high-rise and high-density residental developments in Hong Kong", Energy and Buildings 36, 525- 534

Regentsearth.com. (2017). Cite a Website - Cite This For Me. [online] Available at: http://www.regentsearth.com/ILLUSTRATED%20GLOSSARY/Albedo.htm [Accessed 9 Feb. 2017].

RIZWAN, A., DENNIS, L. and LIU, C. (2017). A review on the generation, determination and mitigation of Urban Heat Island.

Rosenfeld, A.H., Akbari, H., Bretz, S., Fishman, B.L., Kurn, D. M., Sailor, D. and H. Taha, (1995) : Mitigation of urban heat island. Materials, Utility Programs, Updates, Energy and Buildings, 22, p. 255–265.

Rotem-Mindali, O., Michael, Y., Helman, D. and Lensky, I.M. (2015) 'The role of local land-use on the urban heat island effect of Tel Aviv as assessed from satellite remote sensing', Applied Geography, 56, pp. 145–153. doi:10.1016/j.apgeog.2014.11.023.

Sailor, D. J., & Lu, L. (2004). A top-down methodology for developing diurnal and seasonal anthropogenic heating profiles for urban areas. Atmospheric Environment, 38(17), 2737– 2748.

Scott, R. W., & Huff, F. a. (1996). Impacts of the Great Lakes on Regional Climate Conditions. Journal of Great Lakes Research, 22(4), 845–863.

Senanayake, I., Welivitiya, W. and Nadeeka, P. (2013). Remote sensing based analysis of urban heat islands with vegetation cover in Colombo city, Sri Lanka using Landsat-7 ETM+ data. Urban Climate, 5, pp.19-35.

Small, C. "Comparative Analysis of Urban Reflectance and Surface Temperature." Remote Sensing of Environment 104.2 (2006): 168-89.

Stewart, I. and Oke, T. (2012). Local Climate Zones for Urban Temperature Studies. Bulletin of the American Meteorological Society, 93(12), pp.1879-1900.

Streutker, D. (2003) "Satellite-measured growth of the urban heat island of Houston, Texas." Remote Sensing of Environment 85, no. 3 (2003): 282-289.

Streutker, D. R. (2002). A remote sensing study of the urban heat island of Houston, Texas. International Journal of Remote Sensing, 23(13), 2595–2608.

Thegreencity.com. (2017). The Green City » The causes and effects of the Urban heat island Effect. [online] Available at: http://thegreencity.com/the-causes-and-effects-of-the-urban-heat-island-effect/ [Accessed 24 Mar. 2017].

Touchaei, A. G., & Wang, Y. (2015). Characterizing urban heat island in Montreal (Canada)—effect of urban morphology. Sustainable Cities and Society, 19, 395–402.

Ucl.ac.uk. (2017). Prague. [online] Available at: https://www.ucl.ac.uk/ineqcities/atlas/cities/prague [Accessed 7 Feb. 2017].

United Nations, Department of Economic and Social Affairs, Population Division (2014). World Urbanization Prospects: The 2014 Revision, Highlights (ST/ESA/SER.A/352).

Urbangreenbluegrids.com. (2017). Heat | Urban green-blue grids. [online] Available at: http://www.urbangreenbluegrids.com/heat/ [Accessed 24 Mar. 2017].

Voogt, J. a., & Oke, T. R. (2003). Thermal remote sensing of urban climates. Remote Sensing of Environment, 86(3), 370–384.

Voogt, J.A. (2002) Urban Heat Island. In: Encyclopedia of Global Environmental Change. pp. 660–666, ISBN 0-471-97796-9

Voogt, J.A. (2004). Urban heat islands: hotter cities. Retrieved from http://www.actionbioscience.org/environment/voogt.html
Voogt, J.A. and Oke, T.R. (2003) 'Thermal remote sensing of urban climates', Remote Sensing of Environment, 86(3), pp. 370–384. doi: 10.1016/S0034-4257(03)00079-8.

Wang M., (2016). Characterization of Surface Urban Heat Island in the Greater Toronto Area Using Thermal Infrared Satellite Imagery. UWSpace. http://hdl.handle.net/10012/10111

Whitman, S., Good, G., Donoghue, E. R., Benbow, N., Shou, W., & Mou, S. (1997). Mortality in Chicago attributed to the July 1995 heat wave. American Journal of Public Health, 87(9), 1515–1518.

WHO (2015) Urban population growth. Available at: http://www.who.int/gho/urban_health/situation_trends/urban_population_growth_text/en/ (Accessed: 17 February 2017).

WHO (2004) Urban Bioclimatology. Heat-Waves: Risks and Responses, Health and Global Environmental Change Series, No. 2, WHO Regional Office for Europe, Denmark

Wienert U (2001). Untersuchungen zur Breiten- und Klimazonenabhängigkeit der urbanen Wärmeinsel: Eine städtische Analyse. Essen, Fachbereichs Bio- und Geowissenschaften, Landschaftsarchitektur an der Universität Essen (dissertation).

WMO (1983) Abridged Final Report, 8th Session. Commission for Climatology and Applications of Meteorology, World Meteorological Organization (WMO No. 600), Geneva.

Worldpopulationreview.com. (2017). Cite a Website - Cite This For Me. [online] Available at: http://worldpopulationreview.com/world-cities/prague-population [Accessed 11 Jan. 2017].

Yamashita, S., Sekine, K., Shoda, M., Yamashita, K. & Hara, Y. (1986). On relationships between heat island and sky view factor in the cities of Tama river basin, Japan. Atmospheric Enviornment, 20, 681-686.

Yang, J., Wong, M., Menenti, M. and Nichol, J. (2015). Study of the geometry effect on land surface temperature retrieval in urban environment. ISPRS Journal of Photogrammetry and Remote Sensing, 109, pp.77-87.

Yang, L., Qian, F., Song, D.-X. and Zheng, K.-J. (2016) ‘Research on urban heat-island effect’, Procedia Engineering, 169, pp. 11–18. doi:10.1016/j.proeng.2016.10.002.

Yuksel, U.D. (2015) A study on determining and evaluating summertime urban heat islands in Ankara and local scale utilizing remote sensing and meteorological data. PHD thesis.